Lateral current injection GaInAsP/InP laser on semi-insulating substrate for membrane-based photonic circuits

著者	Okumura Tadashi, Kurokawa Munetaka, Shirao Mizuki, Kondo Daisuke, Ito Hitomi, Nishiyama Nobuhiko, Maruyama Takeo, Arai Shigehisa
journal or publication title	Optics Express
volume	17
number	15
page range	12564-12570
year	2009-07-20
URL	http://hdl.handle.net/2297/19580

doi: 10.1364/OE.17.012564

Lateral current injection GaInAsP/InP laser on semi-insulating substrate for membrane-based photonic circuits

Tadashi Okumura,[1,2*] Munetaka Kurokawa,[1,2] Mizuki Shirao, [1] Daisuke Kondo,[1,2] Hitomi Ito, [1,2] Nobuhiko Nishiyama[1], Takeo Maruyama,[3] and Shigehisa Arai[1,2]

[1]*Quantum Nanoelectronics Research Center,Tokyo Institute of Technology,*
2-12-1-S9-5 O-okayama, Meguro-ku, Tokyo 152-8552, Japan
[2]*Dept. of Electrical and Electronic Engineering, Tokyo Institute of Technology,*
2-12-1-S9-5 O-okayama, Meguro-ku, Tokyo 152-8552, Japan
[3]*School of Electrical and Computer Engineering, Kanazawa University,*
Kakuma-machi, Kanazawa, Ishikawa 920-1192, Japan
**tokumura@quantum.pe.titech.ac.jp*

Abstract: A room-temperature pulsed operation was demonstrated using lateral current injection-type lasers composed of a 400-nm-thick GaInAsP core layer with compressively strained 5 quantum wells. A threshold current of 105 mA and corresponding density of 1.3 kA/cm^2 (260 A/cm^2 per well) were obtained with the stripe width of 5.4 μm and the cavity length of 1.47 mm. A fundamental transverse mode operation was obtained with the narrower stripe device of 2.0 μm and the cavity length of 805 μm, while the threshold current and corresponding density were 49 mA and 3.0 kA/cm^2, respectively.

OCIS codes: (140.5960) Semiconductor lasers; (130.3120) Integrated optics devices.

References and links

1. P. Kapur, J. P. McVittie, and K. C. Saraswat, “Technology and reliability constrained future copper interconnects—Part I: Resistance modeling,” Trans. Electron Devices. **49**(4), 590–597 (2002).
2. P. Kapur, G. Chandra, J. P. McVittie, and K. C. Saraswat, “Technology and reliability constrained future copper interconnects.II. Performance implications,” Trans. Electron Devices. **49**(4), 598–604 (2002).
3. D. A. B. Miller, “Rationale and challenges for optical interconnects to electronic chips,” Proc. IEEE **88**(6), 728–749 (2000).
4. G. Chen, H. Chen, M. Haurylau, N. A. Nelson, D. H. Albonesi, P. M. Fauchet, and E. G. Friedman, ““Prediction of CMOS compatible on-chip optical interconnect,” Integr,” VLSI J. **40**(4), 434–446 (2007).
5. R. Nagarajan, M. Kato, J. Pleumeekers, P. Evans, D. Lambert, A. Chen, V. Dominic, A. Mathur, P. Chavarkar, M. Missey, A. Dentai, S. Hurtt, J. Bäck, R. Muthiah, S. Murthy, R. Salvatore, S. Grubb, C. Joyner, J. Rossi, R. Schneider, M. Ziari, F. Kish, and D. Welch, “Single-chip 40-channel InP transmitter photonic integrated circuit capable of aggregate data rate of 1.6 Tbit/s,” Electron. Lett. **42**(13), 771–772 (2006).
6. M. Fujita, R. Ushigome, and T. Baba, “Continuous wave lasing in GaInAsP microdisk injection laser with threshold current of 40 μA,” Electron. Lett. **36**(9), 790–791 (2000).
7. O. Painter, R. K. Lee, A. Scherer, A. Yariv, J. D. O’Brien, P. D. Dapkus, and I. Kim I, “Two-dimensional photonic band-Gap defect mode laser,” Science **284**(5421), 1819–1821 (1999).
8. H.-G. Park, S.-H. Kim, S.-H. Kwon, Y.-G. Ju, J.-K. Yang, J. H. Baek, S.-B. Kim, and Y.-H. Lee, “Electrically driven single-cell photonic crystal laser,” Science **305**(5689), 1444–1447 (2004).
9. C. Seassal, C. Monat, J. Mouette, E. Touraille, B. B. Bakir, H. T. Hattori, J.-L. Leclercq, X. Letartre, P. Rojo-Romeo, and P. Viktorovitch, “InP bonded membrane photonic components and ciricuits: Toward 2.5 dimentional micro-nano-photonics,” IEEE J. Sel. Top. Quantum Electron. **11**(2), 395–407 (2005).
10. T. Okamoto, N. Nunoya, Y. Onodera, T. Yamazaki, S. Tamura, and S. Arai, “Optically pumped membrane BH-DFB lasers for low-threshold and single-mode operation,” IEEE J. Sel. Top. Quantum Electron. **9**(5), 1361–1366 (2003).
11. N. Nunoya, M. Nakamura, M. Morshed, S. Tamura, and S. Arai, “High-performance 1.55-μm wavelength GaInAsP-InP Distributed-Feedback Lasers with wirelike active regions,” IEEE J. Sel. Top. Quantum Electron. **7**(2), 249–258 (2001).

#110433 - $15.00 USD Received 29 Apr 2009; revised 24 Jun 2009; accepted 4 Jul 2009; published 9 Jul 2009

12. S. Sakamoto, H. Naitoh, M. Ohtake, Y. Nishimoto, S. Tamura, T. Maruyama, N. Nishiyama, and S. Arai, "Strongly index-coupled membrane BH-DFB lasers with surface corrugation grating," IEEE J. Sel. Top. Quantum Electron. **13**(5), 1135–1141 (2007).
13. H. Naitoh, S. Sakamoto, M. Ohtake, T. Okumura, T. Maruyama, N. Nishiyama, and S. Arai, "GaInAsP/InP Membrane Buried Heterostructure Distributed Feedback Laser with Air-Bridge Structure," Jpn. J. Appl. Phys. **46**(47), L1158–L1160 (2007).
14. T. Maruyama, T. Okumura, S. Sakamoto, K. Miura, Y. Nishimoto, and S. Arai, "GaInAsP/InP membrane BH-DFB lasers directly bonded on SOI substrate," Opt. Express **14**(18), 8184–8188 (2006).
15. T. Okumura, T. Maruyama, M. Kanemaru, S. Sakamoto, and S. Arai, "Single-mode operation of GaInAsP/InP-membrane distributed feedback lasers bonded on silicon-on-insulator substrate with rib-waveguide structure," Jpn. J. Appl. Phys. **46**(48), L1206–L1208 (2007).
16. H. Namizaki, H. Kan, M. Ishii, and A. Ito, "Transverse-junction-stripe-geometry double-heterostructure lasers with very low threshold current," J. Appl. Phys. **45**(6), 2785–2786 (1974).
17. K. Oe, Y. Noguchi, and C. Caneau, "GaInAsP lateral current injection lasers on semi-insulating substrate," IEEE Photon. Technol. Lett. **6**(4), 479–481 (1994).
18. E. H. Sargent, K. Oe, C. Caneau, and J. M. Xu, "OEIC-enabling LCI lasers with current guides: Combined theoretical-experimental investigation of internal operating mechanisms," IEEE J. Quantum Electron. **34**(7), 1280–1287 (1998).
19. M. Aoki, H. Sano, M. Suzuki, M. Takahashi, K. Uomi, and A. Takai, "Novel structure MQW electroabsorption-modulator/DFB-laser integrated device fabricated by selective area MOCVD growth," Electron. Lett. **27**(23), 2138–2140 (1991).

1. Introduction

Progress in very-large-scale integration (VLSI) technologies has been made with scaling, but interconnection problems such as delay, power consumption, bandwidth, and crosstalk have become prominent recently [1,2]. The performance of VLSI is mainly influenced by its interconnection. One of the promising solutions for this problem is replacing the electrical global wiring within chip or chip-to-chip by an optical interconnection [3,4]. An optical signal system has advantages in terms of the delay because it is independent of the wiring capacity. In addition, high speed and wideband data transmission are expected with the wavelength-division multiplexing (WDM) technique [5]. An ultra low-power consumption light source is essential to utilize the advantage of the optical system in the short-reach optical interconnection. To achieve low threshold operation of a semiconductor laser, some types of lasers, such as a microdisk laser [6] and a photonic crystal laser [7–9], have been reported. With regard to low threshold and high efficiency characteristics, we have demonstrated the GaInAsP/InP membrane distributed-feedback (DFB) laser with a thin semiconductor core layer and low refractive index cladding layers [10]. An optical confinement factor to the active region of the membrane laser is enhanced to approximately 3 times higher than that of conventional double-heterostrucure lasers, because of the high-index contrast between the core and polymer claddings such as benzocyclobutene (BCB) or silicon dioxide. Moreover, the active region volume and mirror loss can be reduced by adopting a DFB laser cavity with wirelike active regions [11]. A lower threshold current operation is expected with these effects. Thus far, a threshold optical pump with power as low as 0.34 mW was realized for a 2.0-μm-wide and 80-μm-long buried heterostructure (BH) device under a room-temperature continuous-wave (RT-CW) condition [12]. In addition, membrane lasers were demonstrated with a photonic, crystal-like air bridge structure [13] or integrated with a silicon on insulator (SOI) waveguide for silicon photonic integrated circuits [14,15]. However, these devices only operated under an optical pumping condition because their cladding layers are insulators. Since an optical field penetration into the cladding layers, conventional double heterostructures with top metal contacts cannot be used. Transverse junction laser [16] or lateral current injection (LCI) structure lasers on a semi-insulating (SI) substrate, as reported by Oe et al. [17,18], are one of the promising candidates for injection-type membrane lasers.

To ensure consistent presentation, broad accessibility, and long-term archiving, please follow these guidelines on presentation.

In this paper, we report the successful operation of LCI lasers, which consist of a thin (400 nm) GaInAsP core layer including compressively strained 5 quantum wells (CS-5QWs) and

#110433 - $15.00 USD Received 29 Apr 2009; revised 24 Jun 2009; accepted 4 Jul 2009; published 9 Jul 2009

are fabricated by three growth steps of a low-pressure organo-metallic vapor-phase-epitaxy (LP-OMVPE) on a Fe-doped SI-InP substrate.

2. Device structure and fabrication

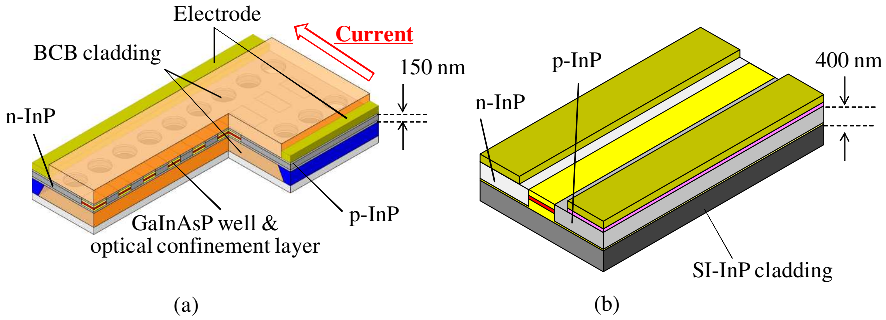

Fig. 1. Illustrations of (a) membrane BH-DFB laser and (b) BH laser on SI-InP substrate.

Our goal is to realize the current injection operation of the membrane DFB laser, as shown in Fig. 1(a). GaInAsP stripes with wirelike active regions are laterally arranged between the buried n-InP and p-InP cladding layers with an air bridge structure. The upper and lower claddings consist of low refractive index materials such as air or BCB. First, we fabricated multiple-quantum-well LCI lasers grown on an Fe-doped SI-InP substrate, as shown in Fig. 1(b). No InP buffer layer was grown on the SI-InP substrate in order to ensure a current injection through the active region in the lateral direction. The initial wafer, consisting of compressively strained 5 quantum wells (CS-5QWs; 6-nm-thick $Ga_{0.22}In_{0.78}As_{0.81}P_{0.19}$ well and 10-nm-thick $Ga_{0.26}In_{0.74}As_{0.49}P_{0.51}$ barrier layers) sandwiched by 155-nm-thick $Ga_{0.21}In_{0.79}As_{0.46}P_{0.54}$ optical confinement layers (OCLs) was grown using LP-OMVPE on an Fe-doped SI-InP substrate, as shown in Fig. 2.

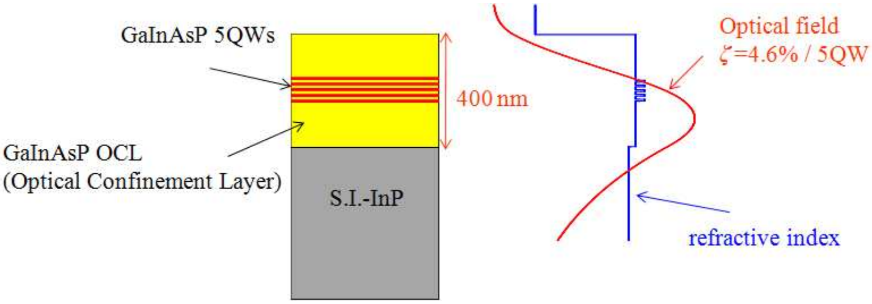

Fig. 2. Wafer structure of the LCI laser and optical field.

All these layers were undoped. The total thickness of these layers was 400 nm, and the optical field profile maxima was slightly (90 nm) shifted downward from the center of the 5QWs structure because of the asymmetric index profile, as shown in Fig. 2. Since the optical confinement factor of the 5QWs structure is calculated to be 4.6%, which is almost comparable to that of the 5QWs structure (5.5%) with 2-µm-thick InP cladding on the top OCL, the threshold current density of around 350 A/cm^2 was expected for the Fabry-Perot cavity lasers, with a cavity length of approximately 1 mm.

#110433 - $15.00 USD Received 29 Apr 2009; revised 24 Jun 2009; accepted 4 Jul 2009; published 9 Jul 2009

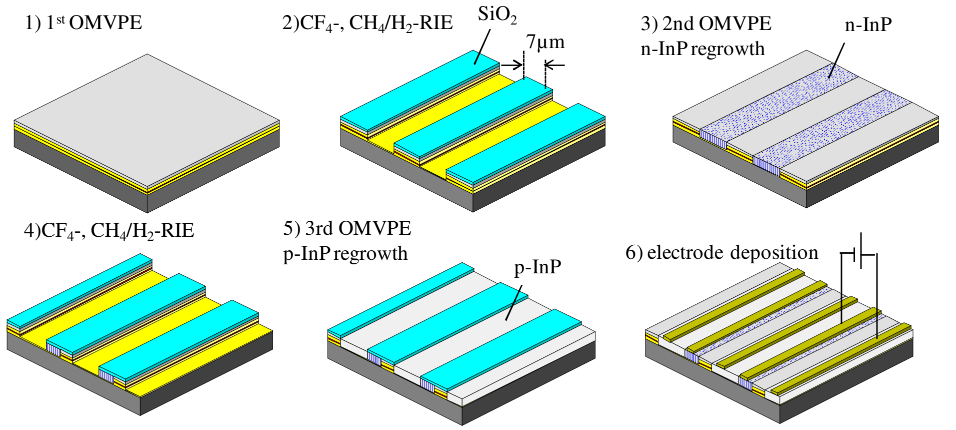

Fig. 3. Fabrication processes of LCI lasers.

Fabrication processes are shown in Fig. 3. First, an initial wafer of the LCI FP laser was prepared using LP-OMVPE on the Fe-doped SI-InP. After depositing 50-nm-thick SiO_2 by plasma-enhanced chemical vapor deposition (PECVD), a 7-μm-wide SiO_2 stripe mask and 380-nm-high mesa structure were fabricated using CF_4 and CH_4/H_2 reactive ion etching (RIE), with an interval of 300 μm. After wet chemical cleaning was performed to remove the damage of the RIE etching interfaces, n-InP was re-grown on both sides of the stripe by the OMVPE, where the growth thickness was controlled to be around 400 nm in order to obtain a flat surface. Next, the part of the wide mesa and one side of the n-type cladding layer were etched with similar processes, except for the SiO_2 stripe mask width of 150 μm, p-InP cladding, and p-GaInAs contact layers, which were re-grown. Finally, both electrodes were formed by evaporating Ti/Au on the resist patterned surface, followed by a lift-off process. We fabricated two types of lasers with different stripe widths of around 5.4 μm and 2.0 μm, where spacings between the p-side and n-side metal contacts were 23 μm and 17 μm, respectively.

3. Device characteristics

Figure 4(a) shows the schematic and cross-sectional SEM view of the sample, with a 5.4-μm-wide stripe. While an almost flat re-grown interface was observed between the n^+-InP and GaInAsP core layers, extraordinarily thick (1.3 μm) p-InP cladding and p-GaInAs contact layers were observed, even though the growth period was reduced to half of that used in the growth of the n-InP cladding layer. This anomalous growth at the edge of the SiO_2 masked region can be eliminated by narrowing the stripe width of the SiO_2 mask [19]. It may also cause a field penetration to the p-type layer. The field penetration to the p-type layer was twice as much as the flat structure. The field overlap with the p-GaInAs layer was calculated to be 0.1%. Figure 4(b) shows the voltage and light output characteristics against the injection current of a FP laser, with the cavity length of 1470 μm under a RT pulsed condition (width 10 μs, repetition 1 ms). The threshold current (I_{th}) of 105 mA and threshold current density (J_{th}) of 1.3 kA/cm^2 (260 A/cm^2/well) were obtained. This value is approximately 3.5 times higher than that of the conventional double heterostructure lasers with the same QW structure. This increase may be attributed to the high waveguide loss because of an overlap of the optical field with the heavily Zn-doped (4×10^{18} /cm^3) p-InP layer. Appropriate Zn doping profile should be found to minimize absorption loss as well as electrical resistance in the future. Figure 4(c) shows far field patterns at a bias current of 300 mA, where the first-order transverse mode operation was confirmed in the horizontal direction (indicated by the blue line) due to oversized stripe width. On the other hand, the far field pattern in the vertical direction shows the reflection from the substrate due to the vertical leaky optical field.

#110433 - $15.00 USD Received 29 Apr 2009; revised 24 Jun 2009; accepted 4 Jul 2009; published 9 Jul 2009

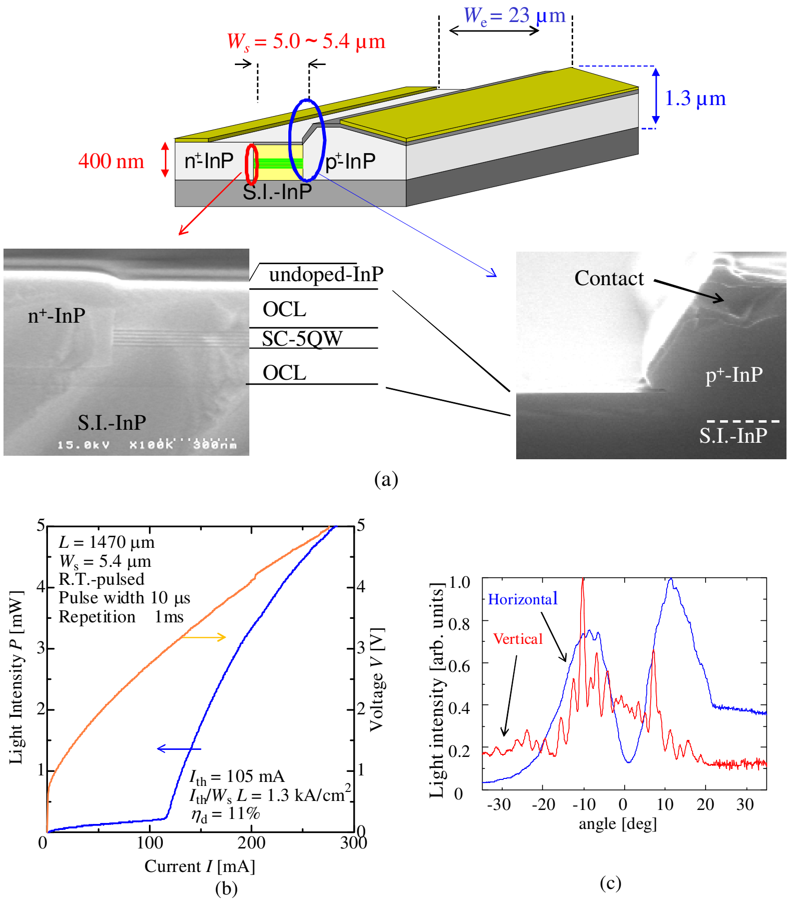

(a)

(b)

(c)

Fig. 4. (a) Schematic structure and cross sectional SEM views of the 5.4-um-wide device (b) I-V, I-L characteristics of 1470 µm long LCI laser (c) Far field pattern of 5.4-µm wide stripe.

Figure 5 shows the cross-sectional SEM view and lasing characteristics of the 2.0-µm-wide stripe laser under RT pulsed conditions (width 1 µs, repetition 1 ms). A threshold current (I_{th}) of 49 mA and threshold current density (J_{th}) of approximately 3.0 kA/cm^2 (600 A/cm^2/well) were obtained for the cavity length of 805 µm. Threshold current density was almost 2.5 times higher than that of the wider stripe device shown in Fig. 4(b), which may be attributed to the shorter cavity length and the lower internal quantum efficiency. From the cavity length dependences of external differential quantum efficiency, waveguide loss and internal quantum efficiency were estimated to be 20 cm^{-1} and 11%, respectively as shown in Fig. 5(c). The high waveguide loss was attributed to the optical absorption of the GaInAs layer because the p-InP overgrowth observed in the 2.0-µm-wide stripe device was somehow suppressed. The p-GaInAs contact layer, which contributes to large optical absorption, was located near the active region. The waveguide loss can be reduced by etching off the GaInAs contact layer in the neighborhood of the active region, while the series resistance will increase in some degree. The design of next devices should be done with the consideration of this tradeoff between the absorption and the resistance. As shown in Fig. 5(d), a far field pattern in the horizontal direction shows a stronger emission for the fundamental mode because of narrower stripe width. However, the stripe width did not satisfy the cut-off condition of higher-order transverse mode.

#110433 - $15.00 USD Received 29 Apr 2009; revised 24 Jun 2009; accepted 4 Jul 2009; published 9 Jul 2009

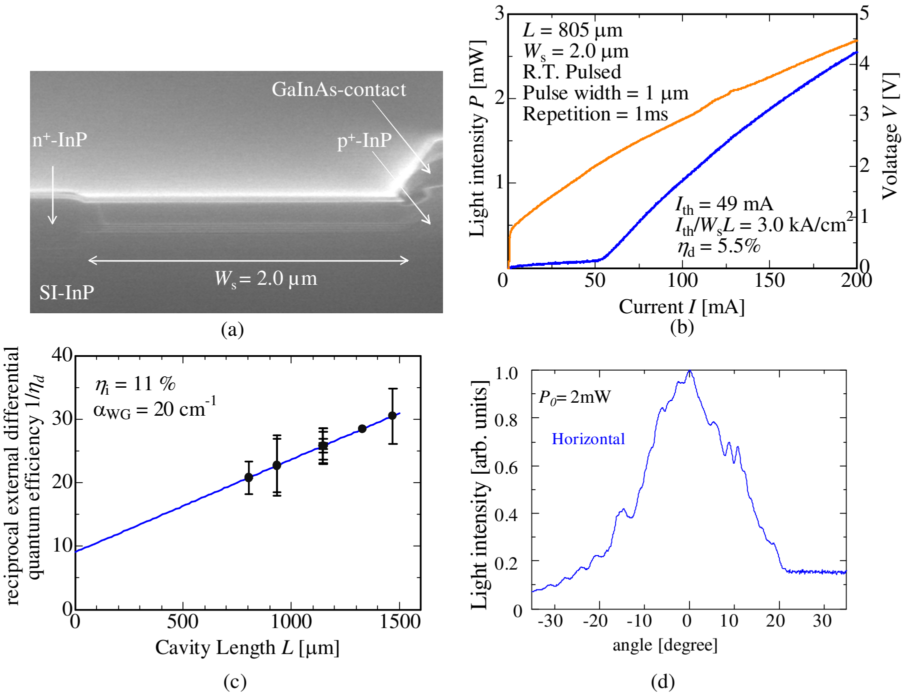

Fig. 5. a) Cross sectional SEM view of 2.0 µm width device (b) I-V, I-L characteristics of 2.0 m width and 805 µm long LCI laser (c) External quantum efficiency as a function of cavity length (d) Far field pattern of 2.0-µm wide stripe.

In particular, the lateral gain profile and carrier injection efficiency to the QWs should be considered for this LCI structure. The difference between the mobilities of electrons and holes may cause a non-uniform optical gain profile. Injected electrons with higher mobility and holes with lower mobility tend to recombine in the GaInAsP active region near the p-InP side. Figure 6 shows calculated relative recombination radiation with a current density slightly below threshold, and is normalized by its peak value. As can be seen, the uniformity of the recombination radiation profile degrades as the stripe width expands because of the poor mobility of holes. Another point to be considered is leakage current flowing inside OCLs and outside QWs. In order to reduce the leakage current, a reduction in thickness and an increase in the bandgap energy of the OCLs are effective to enhance the carrier injection efficiency into QWs.

#110433 - $15.00 USD Received 29 Apr 2009; revised 24 Jun 2009; accepted 4 Jul 2009; published 9 Jul 2009

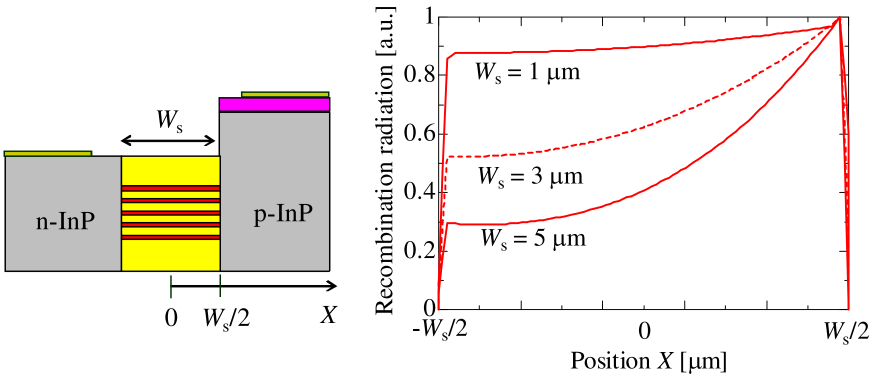

Fig. 6. Simuration model and results of the recombination radiation distribution in latelal direction.

4. Conclusion

A lateral current injection type laser consisting of CS-5QWs with a 400-nm-thick core layer was realized. A threshold current of 105 mA with the stripe width of 5.4 μm and the cavity length of 1.47 mm was obtained, showing that the higher transverse mode operation originates in the wide stripe and lateral current injection structure. In addition, a narrower stripe device was fabricated from the aspect of the fundamental transverse operation. A threshold current of 49 mA and a fundamental transverse mode oscillation were achieved for the stripe width of 2.0 μm and the cavity length of 805 μm. Even though fabrication of the membrane structure and introduction of the DFB grating are required for low-power consumption laser operation, this technology is applicable for the realization of other membrane-based photonic devices and functional photonic integrated circuits.

Acknowledgments

We would like to thank Professors Emeritus Y. Suematsu and K. Iga for their continuous encouragement, and Professors K. Furuya, M. Asada, F. Koyama, K. Kobayashi, T. Mizumoto, Y. Miyamoto, M. Watanabe, T. Miyamoto and H. Uenohara, Tokyo Institute of Technology, for fruitful discussions. This research was partially supported by a Grant-in-Aid for Scientific Research (# 19002009, #19686023, #19760231, and # 20055211) from the Ministry of Education, Culture, Sports, Science and Technology (MEXT), Japan. The first author would like to acknowledge the Japan Society for the Promotion of Science (JSPS) for the Research Fellowship for Young Scientists.

Received 29 Apr 2009; revised 24 Jun 2009; accepted 4 Jul 2009; published 9 Jul 2009